FABRICATION AND SUPERIOR PERFORMANCE OF FLATTENED NETWORK STRUCTURED TIC/TI COMPOSITES

Fengbo Sun[1], Lujun Huang[2] and Lin Geng[3]

[1] School of Materials Science and Engineering, Harbin Institute of Technology, P. O. Box433, Harbin, 150001, PR China, 19b909031@stu.hit.edu.cn

[2] School of Materials Science and Engineering, Harbin Institute of Technology, P. O. Box433, Harbin, 150001, PR China, huanglujun@hit.edu.cn, http://homepage.hit.edu.cn/huanglujun?lang=zh

[3] School of Materials Science and Engineering, Harbin Institute of Technology, P. O. Box433, Harbin, 150001, PR China, genglin@hit.edu.cn, http://homepage.hit.edu.cn/genglin

Keywords: Titanium matrix composites, Titanium carbide, Network structure, Hot extrusion

ABSTRACT

Titanium matrix composites (TMCs) shows great potential in aerospace application. However, hard ceramic reinforcements make the hot working of TMCs challenging. In the present work, large spherical Ti powders were introduced into TiC-reinforced Ti matrix composites to improve the deformability at higher temperatures. This composite showed a flattened network structure after hot extrusion. Plastic deformation of TiC occurred during extrusion. Compared with the composites with homogeneous microstructure, the flattened network structured TiC/Ti composite has higher elastic modulus but lower strength.

1 INTRODUCTION

Titanium matrix composites (TMCs) are promising in the aerospace field due to their high specific modulus, high specific strength, good corrosion resistance, and remarkable high temperature properties below 800 ºC [1,2]. Among these composites, discontinuous reinforced TMCs (DRTMCs) show good isotopy and can be machined into complex shapes [3]. In recent years, considerable attention has been paid to improving the strength and ductility of TMCs. For example, Zhang et al. [4] enhanced the strengthening efficiency of TiBw in a network structured titanium matrix composites by combining solid solution treatment with hot processing. The extra solid strengthening treatment contributed to the microstructure refinement and brought about an improvement of 10% in the yield strength. Ma et al. [5] solve the strength-ductility trade-off using a novel two-step hot isostatic pressing strategy. The yield strength, ultimate strength, and elongation were improved by 9.6%, 11.0%, and 1.9%. These works also prove that an inhomogeneous structure may improve deformability. However, the content of ceramic reinforcement in these composites is generally low, which means the elastic modulus was enhanced finitely. Although elastic modulus is also critical in certain applications, few works focus on DRTMCs with a high fraction of reinforcement. As the increased faction of reinforcement, the comprehension properties decrease severely. Besides, the increased content of reinforcement usually increases the strength at high temperatures, which makes the hot working of these composites challenging. For high-modulus DRTMCs, it is generally difficult to hot process. This problem mainly attributes to the brittle ceramic phase in the composites.

TiB and TiC are always considered the optimal reinforcement in DRTMCs due to their desirable properties [6]. Most of the in situ TiB exhibit as whiskers in DRTMCs. Generally, TiBw is still brittle even in the hot working temperature of DRTMCS. TiBw is easily fractured during hot extrusion, especially when the fraction is high [7]. In the DRTMCs fabricated by powder metallurgy, TiC exhibits ellipse shape [8]. As reported by Das [9], the ductile-brittle transition temperature of TiC was determined to be around 800 ºC in compression. This temperature was lower than some of the hot working temperatures of DRTMCs. Therefore, it could be inferred that TiC may undergo plastic deformation under certain conditions. Wang et al. [10] observed the dislocations in TiC after hot forging, which means that TiC deformed slightly during processing. The observation provides a possible solution for fabricating DRTMCs with better deformability: introducing deformable TiC into DRTMCs.

In order to understand the impact of reinforcements distribution, we fabricated TiC-reinforced titanium matrix composites with different structures. The composites were extruded to compare their thermal processing capabilities. The microstructure and mechanical properties of the as-extruded composites were analysed. This study can provide guidance for the design and hot working of DRTMCs with high elastic modulus.

2 MATERIALS AND METHODS

The raw materials included graphite powder and pure Ti powders (irregular shape, ~35μm) for composites with homogeneous structure. And for the composites with a flattened network structure, 25% of irregular Ti powders were replaced by large spherical pure Ti powders (53~105μm). Both composites were synthesized by the same procedure, which is shown in Figure 1(a). First, the Ti powders were mixed with 5.3 wt.% graphite powder by planetary ball milling. The powders were milled at a speed of 275 rpm for 5 hours under the protection of an argon atmosphere. The mixed powders were then hot pressed at 1300 ºC for 1 h in vacuum (10^{-2} Pa). During this process, a uniaxial pressure of 25 MPa was applied on the mixed powders to promote densification. The composites were cooled within the furnace to room temperature. The microstructures of the as-sintered composites were shown in Figure 1(b). Then, the billets were held at 1200 ºC for 30 min, followed by extrusion with an extrusion ratio of 16:1. The macroscopic morphologies of the as-extruded composites are displayed in Figure 1(c).

The microstructure was observed using an optical microscope (OM, JX-50), and scanning electron microscope (SEM, SUPRA 55 SAPPHIRE). Electron backscattered diffraction (EBSD) examination was carried out to further characterize the microstructure. The results were then analyzed using the software Aztec. The elastic modulus for bulk specimens was measured by the impulse excitation technique (RFDA-HTVP1750C). The cuboid specimens had a dimension of 35 mm × 4 mm ×3mm. The compression test was conducted by a universal testing machine (AGXplus) at a constant crosshead of 0.1 mm/min. Compressive specimens had dimensions of Φ 3 mm × 4.5 mm. For each kind of material, five specimens were used to obtain stable mechanical properties.

3 RESULTS AND DISCUSSION

As shown in Figure 1(b), the phase in dark grey is titanium carbide, and the phase in light grey is pure titanium. The composite fabricated with irregular Ti powders shows a homogenous microstructure, while spherical Ti powders can introduce titanium carbide lean region. The region shows a similar size as the spherical Ti powders, which means that the Ti powders didn’t deform severely during the milling process. In this composite, TiC particles mainly distribute in the TiC-rich region. It can be seen that the volume fraction of titanium carbide nearly achieves 50%, which indicates that the ceramic phase in the composites is actually substoichiometric TiC. The macroscopic morphology shows that the as-extruded composite with an inhomogeneous structure is longer and shows fewer cracks inside. It is easier for the composite with the inhomogeneous structure to hot work.

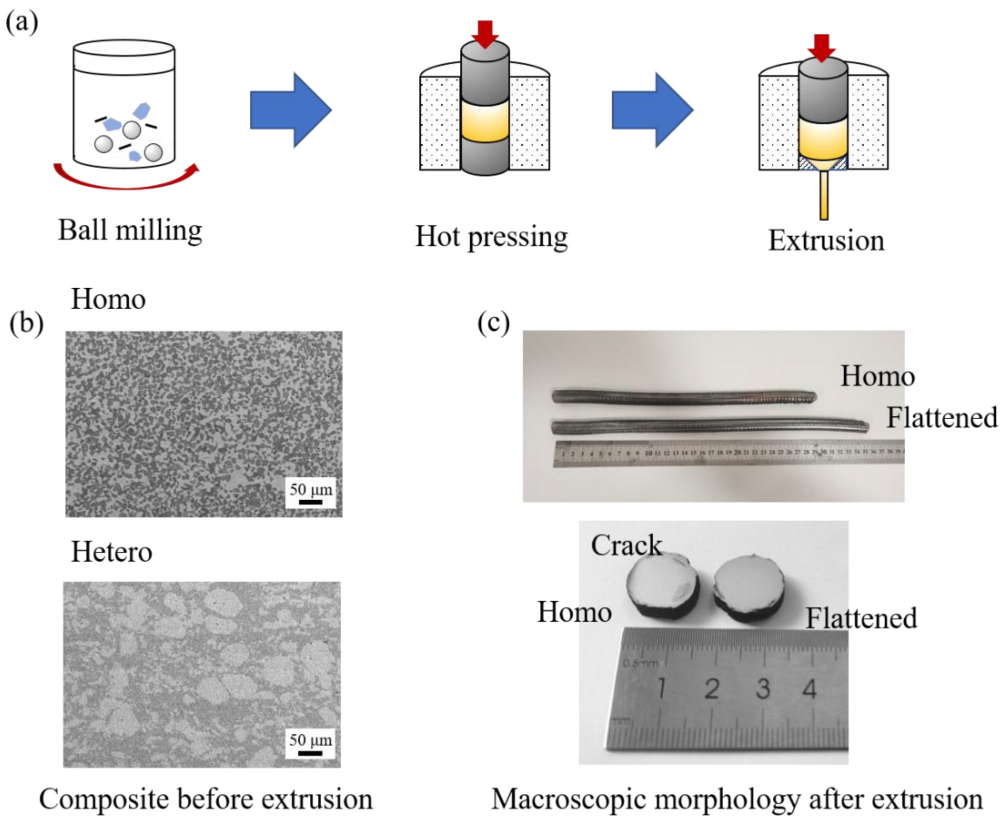

Figure 1: (a) Schematic of the preparation process. (b) Microstructure of composites before extrusion. (c) Macroscopic morphology of composites after extrusion.

In our previous work, the composition of TiC was proved to be $TiC_{0.5}$ in the as-sintered composites [11]. During the sintering process, the following in situ reaction happens:

$$Ti+C \rightarrow TiC_{0.5} \quad (1)$$

Here, to further clarify this process, the Gibbs energy of $TiC_{0.5}$ is considered. According to the Laws of Thermodynamics, the isobaric specific heat capacity (C_p), enthalpy (H), entropy (S), and temperature (T) have the following relationship:

$$C_p = a + b \cdot 10^{-3} T + c \cdot 10^{5} T^{-2} + d \cdot 10^{-6} T^{2} \quad (2)$$

$$H = H_{298} + \int_{298}^{T} C_p dT \quad (3)$$

$$S = S_{298} + \int_{298}^{T} \frac{C_p dT}{T} \quad (4)$$

For each chemical reaction, the variation in Gibbs energy (ΔG) can be expressed as:

$$\Delta G = \Delta H - T \Delta S \quad (5)$$

The thermodynamic data used in this work are listed in Table 1, and the calculated ΔG is shown in Figure 2. From 1173 K to 1673 K, the value of ΔG is approximately -225 KJ/mol. This value is lower than that of the reaction Ti+C→TiC [12], which means $TiC_{0.5}$ is the stable phase in the titanium matrix composites. In the phase diagram of Ti-C [13], titanium carbide shows a wide composition range from $TiC_{0.48}$-TiC. Generally, TiC is used for convenience. In this work, TiC is still used to represent the titanium carbide in the composites.

Phase	Temperature(K)	*a*	*b*	*c*	*d*
Ti	298-1155	22.158	10.284	0	0
	1155-1933	19.828	7.924	0	0
Graphite	298-1100	0.109	38.940	-1.481	-17.385
	1100-4073	24.439	0.435	31.627	0
$TiC_{0.5}$	298-1918	19.88	16.25	28.874	0

Table 1: Selected thermodynamic parameters [13]

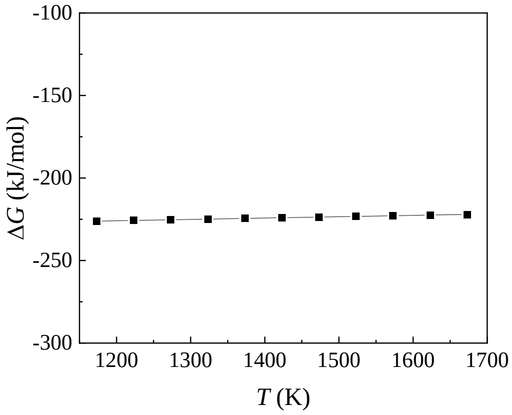

Figure 2: The variation of estimated ΔG over temperature

Figure 3 exhibits the microstructure of the as-extruded composition. In both composites, TiC remains ellipse shape without elongation after hot extrusion. The extrusion process did not change the TiC distribution in the composite with homogeneous microstructure, as shown in Figure 3 (a) and (c). This composite is denoted as Homo-TMC hereafter. However, the large spherical Ti matrix was elongated into a flattened shape (Figure 3(b) and (c)). As TiC shows a flattened network distribution, the composite is then designated as Flattened-TMC.

The band contrast maps in Figure 4 (a) and (b) demonstrate that the particle size of TiC in Flattened-TMC is larger than that in Homo-TMC. Two probable reasons may cause the difference in particle size: On the one hand, the inhomogeneous distribution of TiC shortens the average distance between these particles. TiC mainly concentrates at the boundary of the TiC-lean region. TiC grains could easily grow during sintering, which means the difference in particle size already exists before extrusion. On the other hand, the TiC-lean region shows lower strength compared to the TiC-rich region in Flattened-TMC. During hot extrusion, the TiC-lean region deforms severely, leading to the obvious shape change. As the deformation of the Ti matrix, TiC particles flow. In contrast, Homo-TMC is deformed homogenously during the extrusion process. Stress concentration occurs at the phase boundary, which leads to more particle fracture. This also explains the reason that the deformability of the inhomogeneous composite is better than that of the homogeneous counterpart. Generally, hot extrusion results in strong texture in alloys and their composites. Nevertheless, no obvious texture of TiC or Ti can be observed as shown in the inverse pole figure (IPF) map (Figure 4(b) and (e)). This phenomenon may be attributed to the complicated stress distribution in the composite during extrusion. To understand the evolution of TiC, kernel average misorientation (KAM) maps are displayed in Figure 4(c) and (f). KAM represents the distributions of local orientation gradient, which is related to geometrically necessary dislocation (GND) density distribution [14]. The KAM values prove that TiC deformed plastically in the extrusion process. It is seen that the average KAM values in Homo-TMC are higher than those of Flattened-TMC, which proves the different deformation mechanisms analyzed above. Some small TiC grains with low KAM value appear at the grain boundary of large TiC. These grains arise from dynamic recrystallization behavior. During hot deformation, dislocations in TiC pile up at the grain boundary, which provides energy for recrystallization. Then, the boundary bulges, and new grains form. This behavior is also regarded as discontinuous dynamic recrystallization. This result further proved that plastic deformation of TiC occurs during hot extrusion.

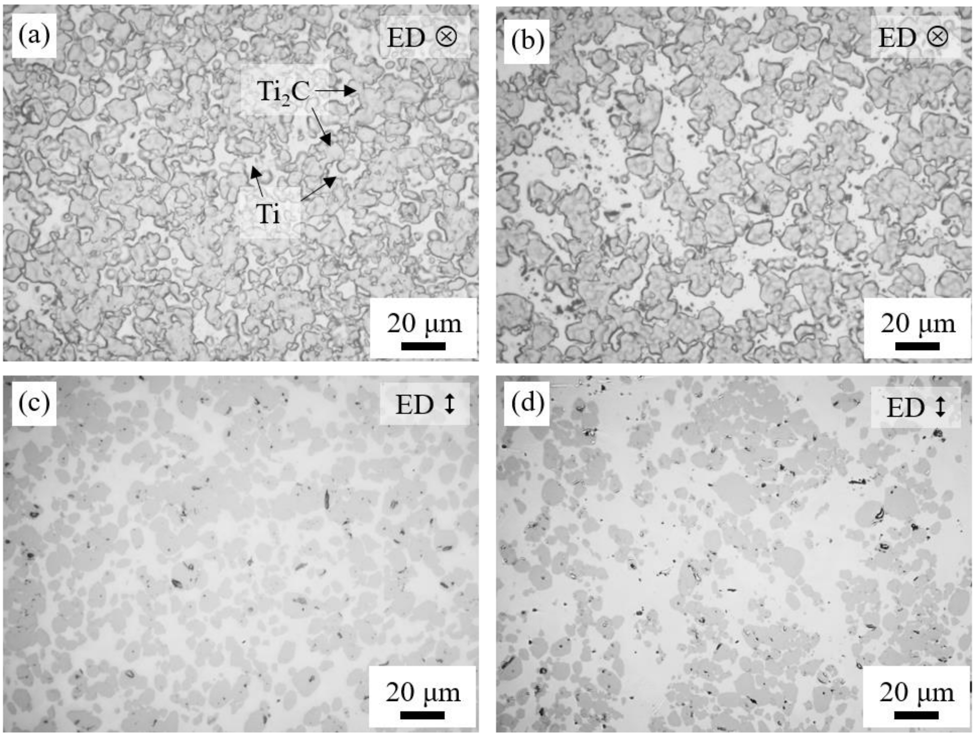

Figure 3. Microstructure of composites with (a, c) homogeneous microstructure and (b, d) flattened network structure after hot extrusion: (a, b) OM images perpendicular to the extrusion direction; (c, d) OM images parallel to the extrusion direction.

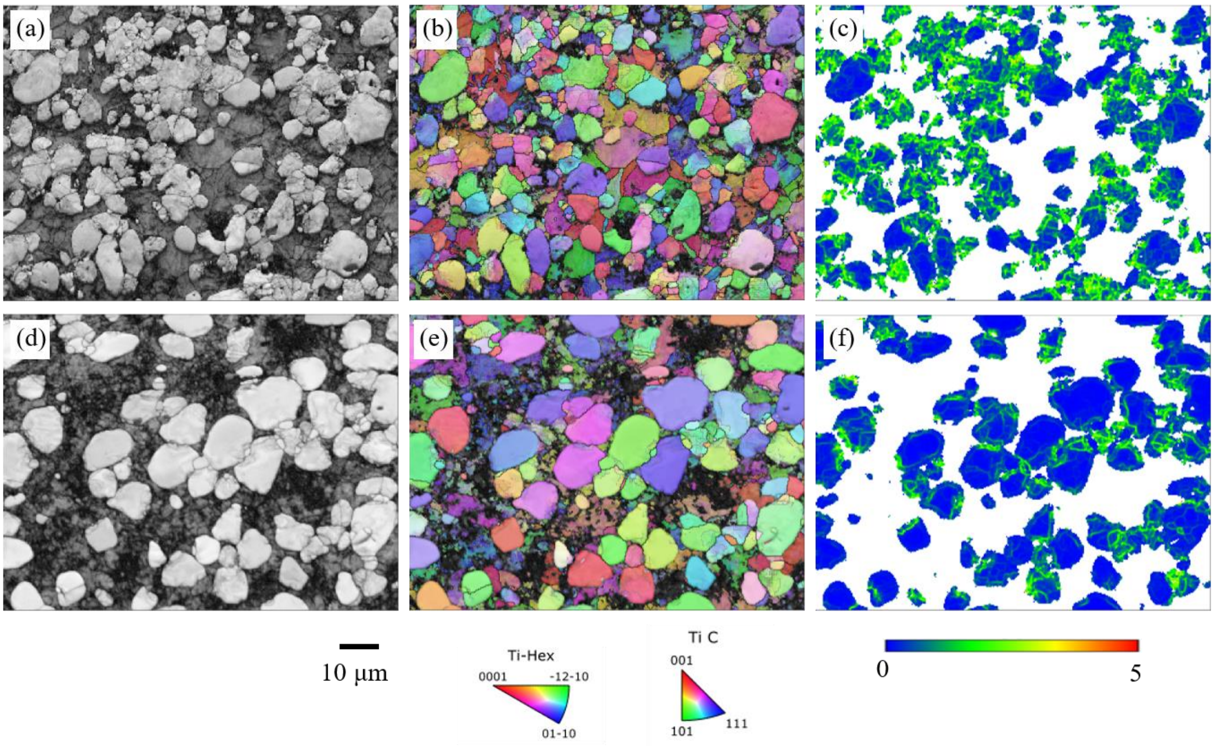

Figure 4. EBSD analysis of (a-c) homogeneous and (d-f) flattened network composites: (a, d) Band contrast images; (b, e) IPF maps; (c, f) kernel average misorientation.

The mechanical properties of both composites are compiled in Table 2 and the compressive stressstrain curves are displayed in Figure 5. The elastic modulus of Flattened-TMC is a little higher than that of Homo-TMC. According to the classical Hashin-Strikman theory [15], the elastic modulus increases as more hard phase connect. The TiC reach region could bearing load effectively in Flattened-TMC. This also explains that most composites with a network structure show a higher elastic modulus [16]. Both the yield strength and ultimate strength of Flattened-TMC are lower than that of Homo-TMC. This phenomenon is mainly attributed to the TiC lean region. Because these regions have lower strength, plastic deformation of Ti first occurs in these regions. Therefore, Flattened-TMCs exhibit lower compressive properties. In both composites, the yield strength and ultimate strength along TD are higher than those of ED. One possible reason is that the Ti matrix still has a preferable orientation in both composites but isn't characterized by the EBSD results. Besides, the fractured TiC and the grain shape of both composites may also impact the strength of the composites. The compressive property needs further analysis and will be discussed in our future work.

	Elastic modulus (GPa)	direction	Compressive yield strength (MPa)	Compressive ultimate strength (MPa)
Homo	168.0	ED	1078±50	1549±50
		TD	1327±37	1687±16
Flattened	170.4	ED	988±10	1385±20
		TD	1116±20	1439±20

Table 2 Mechanical properties

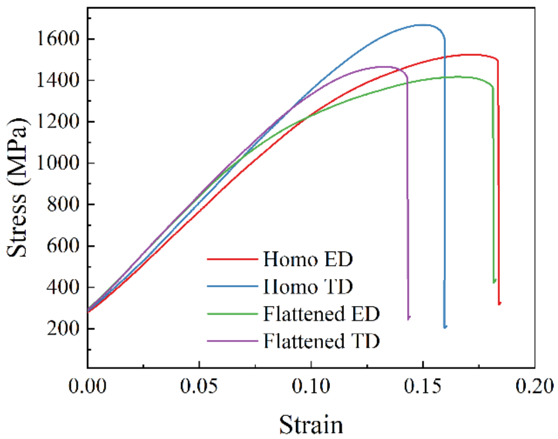

Figure 5. Compressive properties of composites.

4 CONCLUSIONS

(1) According to the Gibbs energy, $TiC_{0.5}$ are preferably formed during sintering.

(2) It was easier to hot extrude composites with large TiC-lean regions.

(3) The composite with TiC-lean region shows a flattened network structure after hot extrusion. Plastic deformation of TiC occurred during hot extrusion.

(4) Due to the flattened network structure, Flattened-TMC shows higher elastic modulus and lower strength compared with Homo-TMC.

ACKNOWLEDGEMENTS

This work is financially supported by National Key R&D Program of China [No. 2021YFB3701203], the National Natural Science Foundation of China [NSFC, grant numbers U22A20113, 52201116, 52071116], Heilongjiang Provincial Natural Science Foundation of China [Grant number TD2020E001], Heilongjiang Touyan Team Program and China Postdoctoral Science Foundation No. 2022M710939.

REFERENCES

[1] S. Wang, Q. An, R. Zhang, S. Jiang, L. Huang, R. Chen, B. Liu, Y. Jiao, L. Geng, Microstructure characteristics and enhanced properties of network-structured TiB/(TA15-Si) composites via rolling deformation at different temperatures, Mater. Sci. Eng. A. 829 (2022). https://doi.org/10.1016/j.msea.2021.142176.

[2] Q. An, L.J. Huang, Q. Qian, Y. Jiang, S. Wang, R. Zhang, L. Geng, L. Wang, Insights into in-situ TiB/dual-phase Ti alloy interface and its high load-bearing capacity, J. Mater. Sci. Technol. 119 (2022) 156–166. https://doi.org/10.1016/j.jmst.2021.12.035.

[3] R. Zhang, L. Huang, X. Zhao, L. Geng, S. Wang, S. Jiang, Y. Jiao, Influence of deformation parameters and network structure to the microstructure evolution and flow stress of TiBw/Ti64 composite, Mater. Sci. Eng. A. 809 (2021) 140997. https://doi.org/10.1016/j.msea.2021.140997.

[4] R. Zhang, S. Wang, W. Lu, F. Sun, L. Huang, L. Bolzoni, L. Geng, F. Yang, Enhancing microstructure refinement and strengthening efficiency of TiBw/near α-Ti composites by combining solid-solution treatment with hot processing, Compos. Part B Eng. 257 (2023) 110696. https://doi.org/10.1016/j.compositesb.2023.110696.

[5] Z. Ma, S. Wang, L. Huang, Q. An, R. Zhang, W. Liu, F. Sun, R. Chen, L. Geng, Synergistically enhanced strength and ductility of TiB/(TA15-Si) composites: A two-step HIP strategy, Compos. Part B Eng. 254 (2023) 1–12. https://doi.org/10.1016/j.compositesb.2023.110583.

[6] Y. Jiao, L.J. Huang, L. Geng, Progress on discontinuously reinforced titanium matrix composites, J. Alloys Compd. 767 (2018) 1196–1215. https://doi.org/10.1016/j.jallcom.2018.07.100.

[7] H.T. Hu, L.J. Huang, L. Geng, C. Liu, B. Wang, Effects of extrusion on microstructure and tensile properties of 3D network structured TiBw/Ti60 composites fabricated by reaction hot pressing, J. Alloys Compd. 582 (2014) 569–575. https://doi.org/10.1016/j.jallcom.2013.08.095.

[8] F.B. Sun, L.J. Huang, R. Zhang, S. Wang, S. Jiang, Y. Sun, Q. An, Y. Jiao, L. Geng, In-situ synthesis and superhigh modulus of network structured TiC/Ti composites based on diamond-Ti system, J. Alloys Compd. 834 (2020) 155248. https://doi.org/https://doi.org/10.1016/j.jallcom.2020.155248.

[9] G. Das, K.S. Mazdiyasni, H.A. Lipsitt, Mechanical properties of polycrystalline TiC, J. Am. Ceram. Soc. (1982) 18–21. https://doi.org/10.1111/j.1151-2916.1982.tb10366.x.

[10] X.Y. Wang, S.P. Li, Y.F. Han, G. Huang, J. Mao, W. Lu, Visual assessment of special rod-like α-Ti precipitates within the in situ TiC crystals and the mechanical responses of titanium matrix composites, Compos. Part B Eng. 230 (2022) 109511. https://doi.org/10.1016/j.compositesb.2021.109511.

[11] F. Sun, S. Wang, X. Chen, R. Zhang, Q. An, W. Liu, L. Huang, L. Geng, Improving flexural strength of Ti2C-Ti cermet by hot compressive deformation: microstructure evolution and fracture behaviors, Sci. China Technol. Sci. 2 (2023). https://doi.org/10.1007/s11431-022-2339-4.

[12] S. Li, B. Sun, H. Imai, T. Mimoto, K. Kondoh, Powder metallurgy titanium metal matrix composites reinforced with carbon nanotubes and graphite, Compos. Part A Appl. Sci. Manuf. 48 (2013) 57–66. https://doi.org/10.1016/j.compositesa.2012.12.005.

[13] A.I. Gusev, Phase equilibria, phases and compounds in the Ti–C system, Russ. Chem. Rev. 71 (2002) 439–463. https://doi.org/10.1070/rc2002v071n06abeh000721.

[14] H. Masuda, E. Sato, Diffusional and dislocation accommodation mechanisms in superplastic materials, Acta Mater. 197 (2020) 235–252. https://doi.org/10.1016/j.actamat.2020.07.042.

[15] Z. Hashin，S. Shtrikman, A variational approach to the theory of the elastic behaviour of multiphase materials, J. Mech. Phys. Solids. 11 (1963). https://doi.org/10.1016/0022-5096(63)90060-7.

[16] L.J. Huang, L. Geng, H.X. Peng, Microstructurally inhomogeneous composites: Is a homogeneous reinforcement distribution optimal?, Prog. Mater. Sci. 71 (2015) 93–168. https://doi.org/10.1016/j.pmatsci.2015.01.002.